# SPECTROGRAPHIC APPROACH FOR DIAGNOSING RF BREAKDOWN IN ACCELERATING RF STRUCTURES

H. Tomizawa[1], T. Taniuchi[1], H. Hanaki[1], Y. Igarashi[2], S. Yamaguchi[2], A. Enomoto[2]

Accelerator Division, Japan Synchrotron Radiation Research Institute (SPring-8)
1-1-1 Kouto, Mikazuki-cho, Sayo-gun, Hyogo 679-5198, Japan[1]
High-Energy Accelerator Research Organization (KEK)
1-1 Oho, Tsukuba, Ibaraki 305-0801, Japan[2]

*Abstract*

The acceleration gradient of an electron linac is limited by rf breakdown in its accelerating structure. We apply an imaging spectrograph system to study the mechanism of rf breakdown phenomena in accelerating rf structures. Excited outgases from the surface emit light during rf breakdown, and the type of outgases depend on surface treatments and rinsing methods for their materials. To study rf breakdown, we used 2-m-long accelerating structures and investigated the effects when high-pressure ultrapure water rinsing (HPR) treatment is applied to these rf structures. We performed experiments to study the outgases emanating from the surface of rf structures with quadruple mass spectroscopy and imaging spectrography of atomic lines. As a result, we could observe instantly increasing signals at mass numbers of 2 ($H_2$), 28 (CO), and 44 ($CO_2$), but not 18 ($H_2O$) just after the rf breakdown. We also conduct spectral imaging for the light emissions from the atoms and ions in a vacuum that are excited by rf breakdown. Using an accelerating structure without HPR treatment, we observed the atomic lines of outgases at 511 nm (Cu I), 622 nm (Cu II), and 711 nm (C I). With HPR treatment, the atomic lines were observed at 395 nm (O I), 459 nm (O II), 511 nm (Cu I), 538 nm (C I), 570 nm (Cu I), 578 nm (Cu I), 656 nm (H: Lyman alpha), and 740 nm (Cu II). In additional surface analysis, it was found that carbon is the most dominant element, with the exception of copper, on the blackened surface of the rf-conditioned accelerating structure without HPR treatment. According to these experiments, we understand that some components of the plasma can affect a copper surface. We also provide a phenomenological review of our experimental results and a simple explanation of rf conditioning with rf breakdown.

## 1 INTRODUCTION

Since particle accelerators were first developed, they have included rf structures to accelerate charged particles due to the fact that accelerating rf structures are demanded for higher-gradient acceleration. The theoretical threshold of rf breakdown derived from the well-known Kilpatrick criterion limits the maximum accelerating field in rf structures. However, under this criterion, only hydrogen was taken into account as a residual gas in rf structures. In reality though, many types of gases may exist as residual gases in a vacuum due to surface treatments and rinsing methods for their materials. A range of contaminants and micron-sized particles may remain on a surface following different treatments. Those contaminants are field emitters, and outgassed due to the rf breakdown in rf structures [1, 2]. According to the works of J. Knobloch and P. B. Wilson, the less outgas and the fewer the contaminating particles, the lower the rf breakdown rate. They proposed the mechanism of generating surface damage with a Helium-adding experiment [1] and a simple model[2]. Their explanations are as follows. An rf breakdown generates the outgas plasma and copper vapour close to the copper surface. This effect excavates a crater by surface heating and melting due to an intense bombardment of the generated plasma ions accelerated by the plasma sheath that separates the body of plasma from the copper surface. The process mentioned above is a mechanism of generating surface damage with craters.

It has been reported that the high-pressure ultrapure water rinsing technique (HPR) is very effective in improving the field gradients for normal conducting and superconducting rf structures [3, 4] because HPR treatment eliminates particle contamination on the surface, which is thought to be one of the causes of field emission. We have a plan to apply this technique to the S-band 2-m-long disk-loaded accelerating structure (see Figure 1).

To study rf breakdown, we use 2-m-long accelerating structures as tested rf structures. Microsecond-pulsed rf power (average accelerating field of 45 MV/m at maximum) is fed into these rf structures. We performed experiments using quadruple mass spectroscopy and imaging spectrography of atomic lines to study the outgases emanating from the surface of rf structures. This imaging spectrograph system is useful for observing irreproducible phenomena such as rf breakdown. Condensed gas and electrons have important roles in triggering the formation of aggressive plasma that acts against the copper surface. In our work, excited neutral and ionised gases in this plasma were observed as atomic lines in the real accelerating structures. Additionally, using XPS, we analysed blackened copper surface of rf-conditioned accelerating structure due to rf breakdown.

In this paper we report the phenomenological review of our experimental results and a simple picture of rf conditioning with rf breakdown.

## 2 EXPERIMENTAL SET-UP

### *2.1 Tested Accelerating structure*

We performed experiments using the high-power test stand at KEK. We chose the two S-band 2-m-accelerating structures with the following fabrication processes:

A. A high-precision turning lathe with a diamond byte machines the accelerating structure's disks and cylinders.
B. The electroplating fabrication method is applied to fix the disks and cylinders together.
C. High-pressure ultra-pure water rinsing (HPR) is applied.

Note that these accelerating structures have a crescent-shaped cut opposite the waveguide iris (see Figure 1) to correct the asymmetry of the electromagnetic fields in coupler cavities.

For comparison, we prepared two different processed accelerating structures with or without HPR treatment ( process C). One of the accelerating structures was rinsed while moving vertically (60 mm/min), orbiting (6.5 rpm) and spraying the pipe with nozzles that jet high-pressure ultra-pure water under optimal conditions [5, 6]. Following to the HPR process, a scroll pump immediately dried the structure, and valves were attached in a clean room. After that, it was evacuated sufficiently by a turbo molecular pump and inserted into a high-power test stand. It is not exposed to the atmosphere after assembly in the clean room.

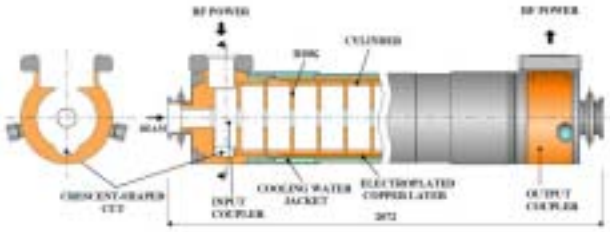

Figure 1: Schematic drawing of the accelerating structure

### *2.2 Imaging Spectrograph System*

#### *2.2.1 Spectrometer and I.I.-camera*

The imaging spectrograph monitor consists of three parts: a spectrometer (SPECIM; ImSpector), an image intensifier (SWAROVSKI; MK500) and a CCD-camera (SONY; Model XC-7500).

The spectrometer was used as an imaging spectrograph that captures a line image and disperses it to a spectrum in a direction orthogonal to the line image. This optics is based on the Prism-Grating-Prism (PGP) technique, which makes a direct-sight imaging spectrograph in which light passes through a straight optical axis. The above configuration offers a combination of several beneficial features:

An astigmatism-free image is available even with a short focal length.

High-efficiency holographic volume diffraction grating and a low f-number produce high throughput.

No reflective surfaces on the optics. The throughput is immune to polarization.

After an image converts to a spectral line image, the image intensifier (I.I.) intensifies the light on the image more than $10^4$ times, making it possible to take a spectrograph of a light emitter with low brightness. The CCD camera then changes intensified spectral line images into video frames with a repetition rate of 30 pps.

All image data were recorded on digital videotapes, because rf breakdown is unpredictable. Each frame contains the line pixels in one dimension (spatial axis) and the spectral pixels in the other dimension (spectral axis), providing full spectral information for each line pixel. It was possible to take spectral information over the entire visible region (380 - 780 nm). The absolute wavelength was calibrated with a He-Ne laser (633 nm) and a mercury lamp (shortest spectral line: 404 nm), while the resolution and geometrical resolution of this spectrograph system were 8.9 nm and 2.4 nm/dot, respectively, over the measured spectral region. Note that, if two spectral lines are separated by more than 8.9 nm, the wavelength accuracy of the spectral peaks is 2.4 nm.

Figure 2: Spectrometer and I.I.-camera for the imaging spectrograph

#### *2.2.2 Data analysing System*

The system of data acquisition and analysis was specially developed for this imaging spectrograph. The vertical and horizontal axes of imaging spectrograph (upper right in Figure 3) represent spatial position and wavelength, respectively. This system enables us to analyse raw video data with a Windows-XP computer (CPU: 2.8 GHz-Pentium4, RAM: 1 GB, Video capture board: Matrox CORONA2), and in addition, it can take data directly form a CCD-camera or a video player and analyse them in real time. It automatically searches video frames for rf breakdown phenomena. The frames are displayed on the screen in the "Random Access" section (see the centre-right in Figure 3). The selected frames with rf breakdown are then sorted into two different groups: "Luminescence Frame" and "Projection Frame". Those frames belonging to the "Luminescence Frame"

group are frames that have one pixel that is brighter than the threshold level. The frames belong to the other group, “Projection Frame”, are those that have an integrated pixel brightness along the vertical axis greater than the threshold level. Both thresholds are determined by background noise on the video images. In this experiment, most of the “Luminescence” and “Projection” frames were full of radiation noise and light emission in the rf breakdown phenomena, respectively. We chose the frames of the “Projection” group and studied their spectra.

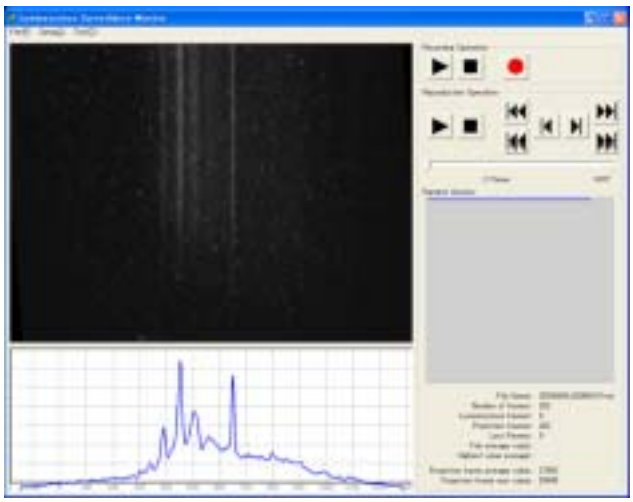

Figure 3: GUI (on Windows XP) of the data analysing system for imaging the spectrograph

### *2.3 Experimental Setup in High-power test stand*

We constructed a test stand for high-power tests on the accelerating structures (Figure 4). A klystron with a maximum peak rf power of 45 MW was used, and a SLED-type pulse compressor to generate a high-power rf pulse was installed in the stand. The pulse width and repetition rate of the rf pulse were 4.0 μsec and 50 Hz, respectively, and the klystron output power level was gradually increased. The reflection of the rf power from the accelerating structure, or waveguides, and the vacuum pressure of the ion pumps (IP in Figure 5) were used as an interlock to stop the rf power. The vacuum pressure of the accelerating structure was maintained at around $1 \cdot 10^{-6}$ Pa during rf conditioning.

We installed a quadruple mass spectroscopy (QMS in Figure 5) and an imaging spectrograph system (S in Figure 5) to study the outgases released from the surface of accelerating structures during rf conditioning. We measured the outgases due to rf breakdown with a quadruple mass spectroscopy (ABB Extrel: Type MAX-200) fitted with four 19-mm diameter mass filter poles; such a large pole diameter was chosen for its higher sensitivity.

We additionally installed the imaging spectrograph camera to directly view the crescent-shaped cuts in the coupler cavities. We supposed that these were some of the most likely locations for rf breakdown to frequently occur, because the surface current densities at these locations are 10 times higher than other surfaces [6]. We often observed some blacked area damaged by rf breakdown in this crescent-shaped cut.

The main difficulty to utilize this optics is how the homogenised laser profile transports toward the cathode surface with focusing. Even if the whole wave front of laser does not reach on the cathode at the same time, the laser spot on the surface should be in the depth of a focus.

Figure 4: High-power test stand at KEK: The camera system is installed downstream to take spectrographs of light emitted due to rf breakdown.

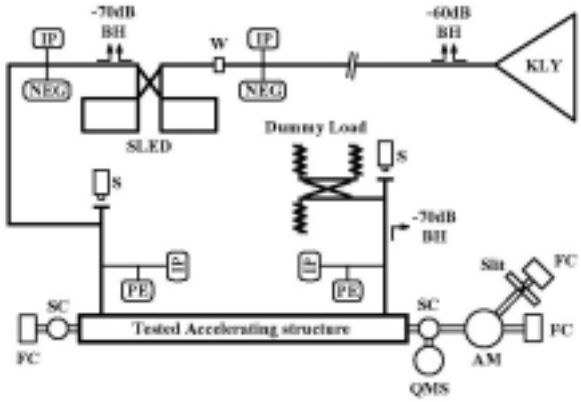


Figure 5: Rf breakdown diagnostic set-up for accelerating rf structure at KEK (KLY: klystron, BH: Bethe hole coupler, IP: ion pump, W: rf-window, SLED: SLED-type pulse compressor, PE: Penning vacuum gauge, SC: screen monitor, FC: Faraday cup, QMS: quadruple mass spectrometer, AM: analyser magnet)

## 3 EXPERIMENTAL RESULTS

### *3.1 Spectrographs of the accelerating structure without HPR*

The initial test was carried out in the accelerating structure but without HPR treatment. After the rf conditioning, an average accelerating field of 40 MV/m was obtained after $1.0 \cdot 10^{8}$ shots (542 hours). Also, the high-power test was terminated due to a time limit. The system experienced 4559 trips due to interlocks with VSWR, which measures rf reflection due to rf breakdown

in the accelerating structures. An imaging spectrograph and the light spectrum of light emission on an rf breakdown are shown in Figure 6 and 7, respectively. Figure 7 clearly shows the atomic lines from outgassed atoms at 711 nm (C I), and evaporated copper at 515 nm (Cu I) and 622 nm (Cu II).

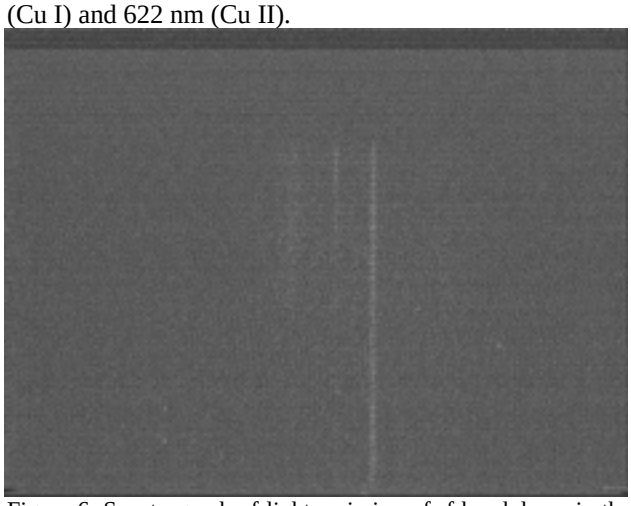

Figure 6: Spectrograph of light emission of rf breakdown in the accelerating structure without HPR treatment (After rf conditioning; elapsed time: 631 hours; average accelerating field: 30 MV/m)

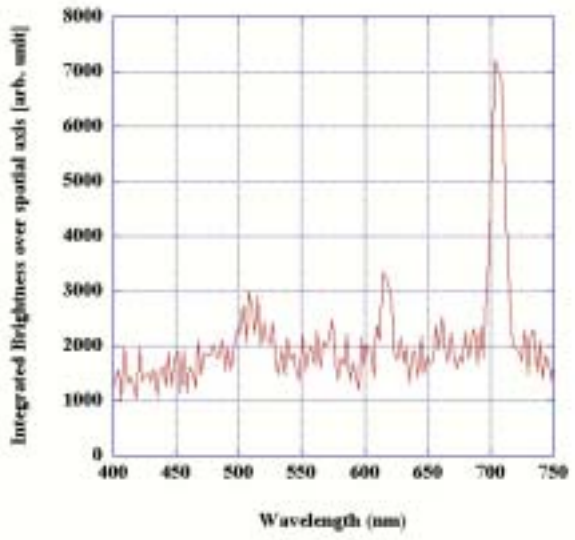


Figure 7: Light spectrum of light emitted due to rf breakdown

## *3.2 Spectrographs of the accelerating structure with HPR*

The next test was carried out using the accelerating structure with HPR treatment (average water pressure: 5.0 MPa). After the rf conditioning, an average accelerating field of 45 MV/m was obtained after $6.4 \cdot 10^7$ shots (356 hours). Although this gradient was limited by the klystron output power. The system experienced 1894 trips due to interlocks with VSWR. Figures 8 and 9 show two imaging spectrographs at elapsed times of 307 (during rf conditioning) and 677 (after rf conditioning) hours, respectively. Figure 8 shows the atomic lines at 395 nm (O I), 511 nm (Cu I), 570 nm (Cu I), 578 nm (Cu I), 740 nm (Cu II), and the most dominant lines at 459 nm (O II) and 656 nm (H: Lyman alpha). In Figure 9 just 538 nm (C I), 656 nm (H: Lyman alpha) and 740 nm (Cu II) were observed; after rf conditioning (elapsed time: 677 hours), we observed only these three lines. On examining rf breakdown over three frames, we found that the 740-nm-line glows first, and then the 656-nm-line glows in the next frame.

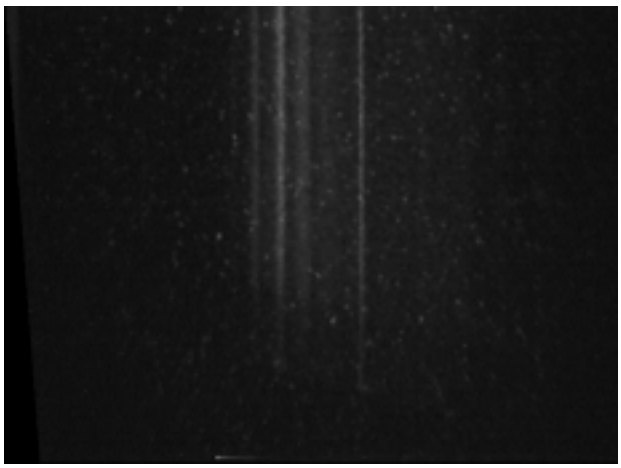

Figure 8: Spectrograph of the accelerating structure with HPR treatment (During rf conditioning; elapsed time: 307 hours; average accelerating field: 42 MV/m)

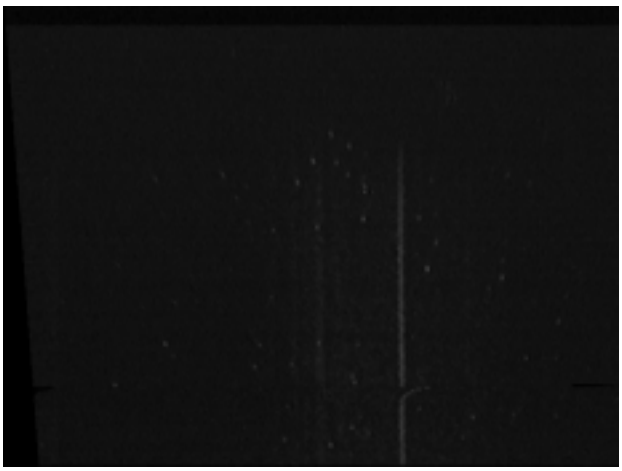

Figure 9: Spectrograph of the accelerating structure with HPR treatment (After rf-conditioning; elapsed time: 677 hours; average accelerating field: 45 MV/m)

## *3.3 The results of analysis on outgases and surface of the accelerating structures*

As a result of the outgas analysis, we could observe instantly increasing signals at mass numbers of 2 ($H_2$), 28 (CO), and 44 ($CO_2$), but not 18 ($H_2O$) (see Figure 10) just after rf breakdown in the accelerating structures. The mass spectrum without rf power is not significantly different form the spectrum before rf breakdown.

In addition, an XPS surface analysis was performed on blackened areas of the crescent-shaped cuts in the coupler

cavities (without HPR treatment), and it was found that carbon (graphite) was the most dominant element, except copper, on the blackened surface of rf-conditioned surfaces.

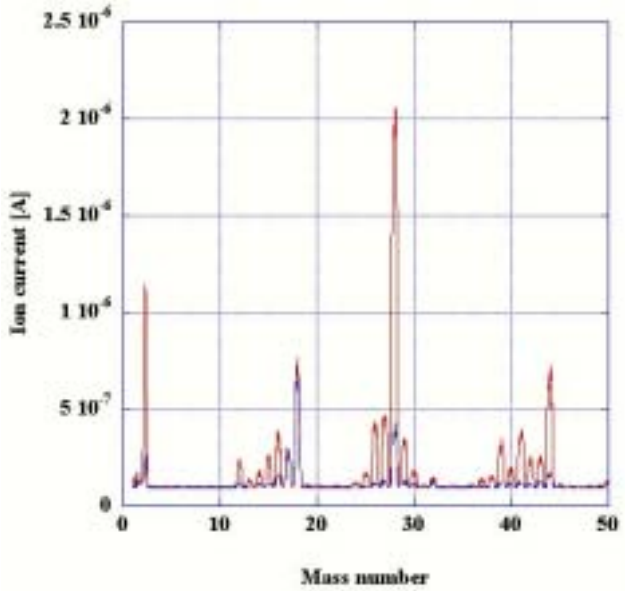


Figure 10: Experimental results of Q-mass: The datum (red solid line) was taken at the same time as the imaging spectrograph shown in Figure 8. The datum (blue solid line) is the mass spectrum before this rf breakdown. The mass spectrum without rf power is not significantly different form the spectrum before rf breakdown.

## 4 SUMMARY

We performed experiments to study the outgases emanating from the surface of rf structures by employing quadruple mass spectroscopy and imaging spectrography of atomic lines. This spectrographic method proved to be particularly useful for observing irreproducible instantaneous phenomena such as rf breakdown. Generally, in both of the accelerating structures, we could observe increasing quantities of $H_2$, CO, and $CO_2$ molecules immediately after the rf breakdown. These molecules could either emanate from the surface or be generated in recombination plasma induced by rf breakdown. According to the spectrographs of this recombination plasma, we mainly observed atomic lines of evaporated copper. Using an accelerating structure without HPR treatment, we observed that the atomic carbon line was the most intense, but no oxygen was detected. On the other hand, with HPR treatment, the atomic oxygen and hydrogen (the most intense) lines were observed in the early stages of rf conditioning; in fact, micro-sized carbon dust particles were present.

According to our experimental results, HPR treatment can remove dust particles, although it causes different contaminant layers to form on the copper surface of the accelerating structure. One of these layers could be a thin oxidized layer, because an oxygen line glows in the early stages of rf conditioning, but not after rf conditioning. This indicates that by the end of rf conditioning, the copper surface of the accelerating structure could become almost oxygen-free, Since an oxidized layer is insulator, ion bombardments can be concentrated on the oxidized layer. Consequently, after rf conditioning, oxygen lines were not observed.

Comparing the two accelerating structures with different processes, we found that the structure using the HPR process reached 45 MV/m with an rf-conditioning period 1.5-times shorter, a lower rf breakdown rate, and a lower dark current than the one that didn't (see reference [6] for more details). Furthermore, the results indicate that the HPR treatment and rf conditioning process help each other to remove contaminants from the surface.

We observed blackened areas damaged by rf breakdown in these crescent-shaped cuts of the rf conditioned accelerating structures with and without HPR treatment. Therefore, we investigated elements of a blackened area on the surface of an rf conditioned accelerating structure without HPR treatment as an example. As a result, the most dominant element, with the exception of copper, on the blackened surface was carbon (graphite). We supposed that carbon ions in plasma recombine with electrons on the copper surface due to the much higher electron density and low electron temperature in the material than in the vacuum. Fortunately, graphite is a conductor. Therefore, if the surface is ideally smooth, it cannot emit a field to initiate rf breakdown.

## 5 ACKNOWLEDGMENT

The authors wish to thank the members of the KEKB Injector for their help. We also acknowledge Dr. K. Saito for advice about the HPR process. In particular, we offer our deepest thanks to the members of the development team at KAWASAKI STEEL Techno-research Corporation. Messrs. S. Moriya, T. Akiyama, H. Fukuda developed and calibrated the imaging spectrograph system.

## 6 REFERENCES

[1] J. Knobloch, "Advanced Thermometry Studies of Superconducting Radio-Frequency Cavities", Ph.D. thesis, Cornell University, August 1997.

[2] P.B. Wilson, Proceedings of the 20th Int. Linear Accelerating Conference, 21-25 August 2000, LINAC2000, Monterey, pp. 618-620.

[3] K. Saito, H. Miwa, K. Kurosawa, P. Kneisel, S. Noguchi, E. Kako, M. Ono, T. Shishido, and T. Suzuki, Proceedings of the 6th Workshop on Superconductivity, 4-8 October, 1993, CEBAF, Newport News, USA, pp. 1151-1159.

[4] M. Yoshioka, H. Matsumoto, Y. Takeuchi, K. Saito, H. Akiyama, E. Tanabe, K. Nishitani, H. Miwa and T. Suzuki, Proceedings of the 17th International Linac Conference, 1994, Tsukuba, Japan, pp. 302-304.

[5] Y. Igarashi, S. Yamaguchi, A. Enomoto, T. Oogoe, K. Kakihara, and S. Ohsawa, Proceedings of the 21th Int.

Linear Accelerator Conference, 19-23 August, 2002, Gyeongju, Korea, in printing.

[6] Y. Igarashi, S. Yamaguchi, A. Enomoto, T. Oogoe, K. Kakihara, S. Ohsawa, H. Tomizawa, T. Taniuchi, and H. Hanaki, Proceedings of the 2003 Particle Accelerator Conference, 12-16 May, 2003, Portland, Oregon, in printing.